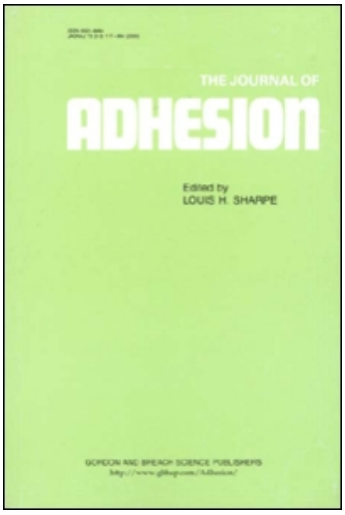

The Journal of Adhesion
Publication details, including instructions for authors and subscription information:
http://www.informaworld.com/smpp/title~content=t713453635

Atomic Force Microscope Techniques for Adhesion Measurements

D. M. Schaefer[a]; J. Gomez[b]
[a] Department of Physics, Astronomy and Geosciences, Towson University, Towson, MD, USA [b] Dept. Fisica de la Materia Condensada, Universidad Autonoma de Madrid, Madrid, Spain

To cite this Article Schaefer, D. M. and Gomez, J.(2000) 'Atomic Force Microscope Techniques for Adhesion Measurements', The Journal of Adhesion, 74: 1, 341 — 359
To link to this Article: DOI: 10.1080/00218460008034535
URL: http://dx.doi.org/10.1080/00218460008034535

J. Adhesion, 2000, Vol. 74, pp. 341–359
Reprints available directly from the publisher
Photocopying permitted by license only

Atomic Force Microscope Techniques for Adhesion Measurements

D. M. SCHAEFER[a,*] and J. GOMEZ[b]

[a]*Department of Physics, Astronomy and Geosciences, Towson University, Towson, MD 21252, USA;* [b]*Dept. Fisica de la Materia Condensada, Universidad Autonoma de Madrid, 28049-Madrid, Spain*

(Received 7 June 1999; In final form 10 September 1999)

The Atomic Force Microscope (AFM) has become a powerful apparatus for performing real-time, quantitative force measurements between materials. Recently the AFM has been used to measure adhesive interactions between probes placed on the AFM cantilever and sample surfaces. This article reviews progress in this area of adhesion measurement, and describes a new technique (Jump Mode) for obtaining adhesion maps of surfaces. Jump mode has the advantage of producing fast, quantitative adhesion maps with minimal memory usage.

Keywords: Adhesion maps; Atomic force microscopy; Force curves; Jump mode

I. INTRODUCTION

The ability to measure interaction forces between an Atomic Force Microscope [1] probe and a surface was exploited shortly after the invention of the AFM. Examples of these forces include electrostatic [2], magnetic [3], double layer [4], van der Waals [5], and frictional forces [6]. Of particular interest to this discussion is the ability of the AFM to measure the force of adhesion between the probe and substrate [7, 8]. Such measurements have been performed on a wide range of conducting and insulating materials [9] in a variety of media,

*Corresponding author. Tel.: 410 830 3007, Fax: 410 830 3511, e-mail: dschaefer@towson.edu

including UHV [10], ambient [11], and liquid [12] environments. Initially, the high force resolution was exploited to produce three-dimensional topographical images of a sample surface. To optimize the lateral resolution during such imaging, sharp probes were used. Recently, however, researchers have modified the AFM probes in order to study specific probe/substrate interactions. By placing a well-characterized micrometer – size sphere on the end of the AFM cantilever, surface force interactions between the sphere and atomically-flat substrates have been reported [13]. Parameters such as lift-off force and work of adhesion have been investigated as a function of applied load. These studies have allowed researchers to investigate the effects of surface roughness and environmental conditions on the measured adhesive force [14]. Additionally, molecular interactions have been studied using the AFM [15]. The force needed to separate individual molecules between functionalized AFM probes and substrates demonstrate the possibility of sensors with single-molecule recognition capabilities.

The following article describes an application of the AFM that combines the high-resolution imaging ability with force measurement. Performing force measurements at various points on a surface provide images representing surface topography, stiffness, and adhesion.

II. FORCE MEASUREMENTS WITH AFM

All quantitative force data derive from a force measurement that results in a force *vs.* displacement curve. Figures 1 and 2 illustrate how force measurements are performed between an AFM probe and a surface. The probe and the surface are brought into close proximity using a coarse approach mechanism. For most force measurements, the probe position is initially several hundred nanometers above the surface. The substrate is then moved toward the probe in a controlled way using a piezoelectric tube. The interaction between the probe and the substrate is monitored by sensing the deflection of the cantilever. Knowledge of the spring constant allows a conversion from cantilever displacement into force. A representation of the force exerted on the probe as a function of substrate displacement is shown in Figure 2. As the probe is brought close to the substrate, any forces acting between the probe and

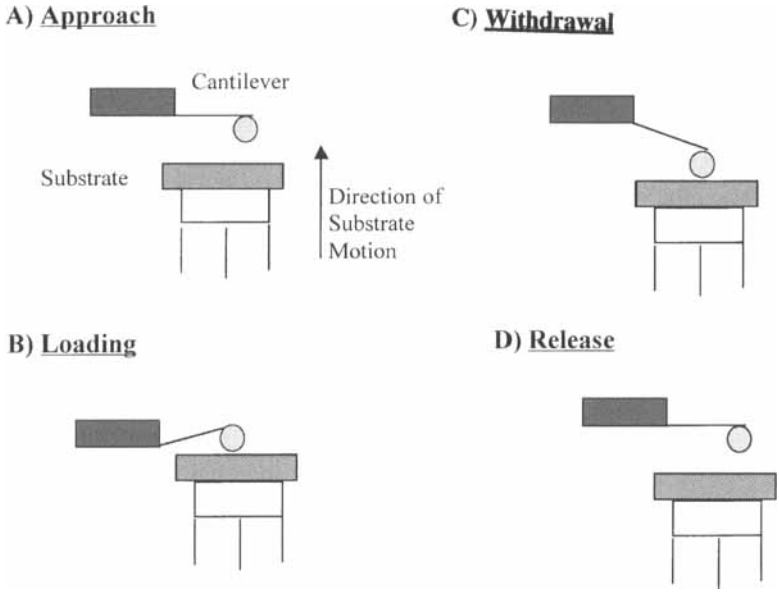

FIGURE 1 Schematic illustrating the process of force measurement with the AFM.

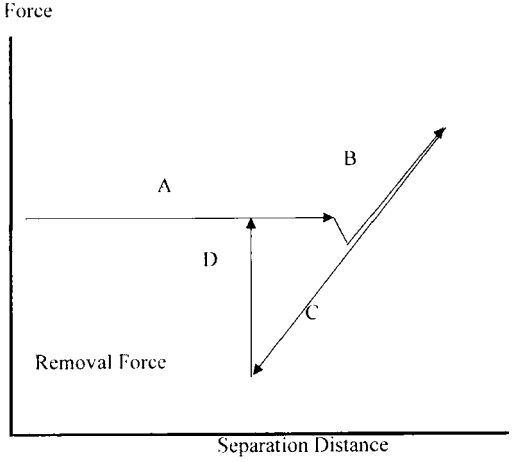

FIGURE 2 Typical shape of the force curve obtained using the AFM.

substrate causes a deflection of the cantilever. The distance-dependence of this deflection is useful for identifying the origin of the interaction force. When the tip is only a few tens of nanometers from the substrate,

an instability occurs. The cantilever flexes and the probe jumps into contact with the substrate. The sample is continually moved forward until a specified positive load is applied by the probe onto the substrate (Fig. 1B). The sample is then withdrawn (Fig. 1C) at the same rate as the approach rate. During unloading, the cantilever motion initially retraces the loading curve (for elastic materials). However, due to binding forces along the contact region, the probe may not separate from the substrate at the same point where contact was originally established. Rather, a substantially larger negative load is required before an abrupt separation occurs (Fig. 1D). This force is the removal force, or adhesion force.

Schaefer *et al.* [16] studied the adhesive forces by systematically measuring the force required to remove different particles from a variety of substrates. In this study, the relative lift-off forces were found to scale consistently with the relative works of adhesion in a manner qualitatively consistent with the predictions of Johnson, Kendall and Roberts (JKR) theory of adhesion [17]. The absolute magnitude of the lift-off force was found to be smaller than expected. This effect was attributed to surface roughness of the particle. Although this study was confined to well-characterized, spherical particles and atomically-flat substrates, the results obtained indicate that the AFM techniques developed are capable of providing useful, quantitative information about the particle adhesion that is difficult to obtain using more conventional techniques.

III. ADHESION MAPS

A natural extension of the previous results is to measure the lift-off force as a function of sample location between the AFM cantilever and a substrate. Figure 3 illustrates the method of producing these adhesion maps. The probe, placed on the AFM cantilever, is raster-scanned from point to point in an $n \times n$ array across an area of the surface. At each point in the array, the surface topography is determined and plotted using the usual false color techniques. A force curve is also taken at each point, and the lift-off force is determined from the minimum of the retrace curve. This force is then plotted using the same false coloring techniques as employed for the topography scans.

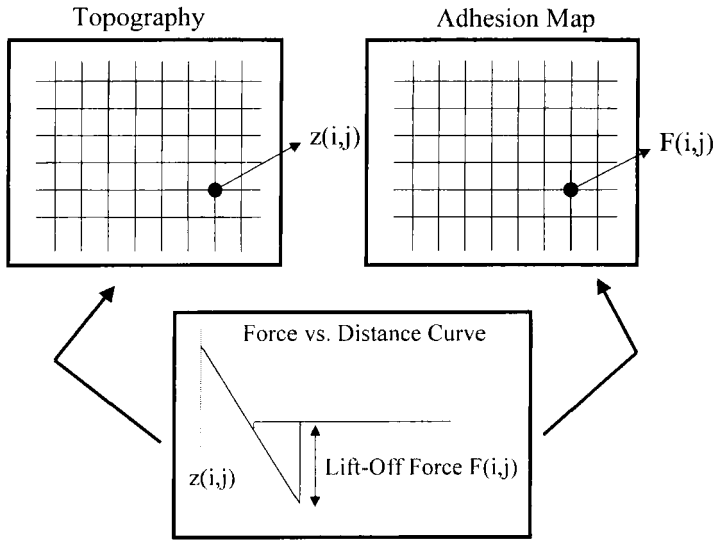

FIGURE 3 Schematic of an adhesion map showing how the topography and adhesion of the tip to the substrate are measured simultaneously.

Different measuring modes have been developed to study the spatial dependence of the adhesion force. Mizes *et al.* [18] first used a commercial AFM to spatially map the adhesion force between a bare Si_3N_4 tip and doped and undoped polycarbonate films. In this study, individual force curves were taken at each imaging point on the sample. A computer algorithm processed each force curve in real time and stored only the minimum of the retrace curve. Adhesion measurements were demonstrated to be repeatable to within 2% when taken over the same region of the sample. It was noted that this result conflicts with macroscopic measurements where repeated contacts cause charge transfer and an associated increase in adhesion due to Coulombic attraction. Mizes argued that the enhanced adhesion is not seen at the microscopic scale because (1) triboelectric charging does not contribute significantly to the adhesive force at this scale, (2) all the tribocharging occurs with first contact, or (3) the sample is slightly conducting over the whole surface between contacts. Experiments by Gady [12, 19, 20] have shown that the charge on a particle attached to an AFM cantilever will increase with increasing contact. This would suggest that (2) is not responsible for the repeatability.

Additionally, experiments by Schaefer [21] have demonstrated that charging can play a significant role in adhesion force for large charge densities. The amount of charge accumulated on the AFM tip during Mizes' experiments, however, would probably be sufficiently small such that charging would not significantly contribute to the adhesive force. For larger scan sizes, the adhesion force was shown to vary from 0.76 to 3.63 mdyn. This variation was explained by proposing a changing contact area between tip and surface due to topographic variations.

Koleske *et al.* [22] utilized a similar technique to obtain adhesion maps using a home-built system. In this technique the entire force curve was taken at each point and stored in computer memory. Adhesion forces were determined in post-acquisition processing. The major disadvantages of performing force mapping in this way are the extensive data storage space necessary and the time for imaging. In the studies by Mizes, 2×2 micron scans are reported to take 40 minutes, and Koleske reports that a 256×256 pixel image (1500 nm $\times$ 1500 nm) taken on a 2400 line/mm grating spanned 4 hours. As observed by Koleske, the effects of thermal and piezoelectric drift can become significant over these time scales.

The effects due to long imaging times were eliminated by van der Werf *et al.* [23] by using analog electronics to control the tip motion and record topography and adhesion information. Detection electronics were used to determine the sample topography, the minimum value of the withdraw curve (removal point), the width of the removal trace, and the area of the adhesion trace. Adhesion maps were obtained in air and liquid, with force curves taken at a rate of 550 Hz (air) and 70 Hz (liquid). Thus, in air, the time for the adhesion map to be completed would be on the order of a few minutes. Van der Werf was able to use this apparatus to show the effects of humidity on the adhesive force in air. By comparing the adhesive force between a Langmuir-Blodgett monolayer film (DPDA) placed on a glass slide with the adhesive force of the bare glass substrate, it was shown that the adhesive force on the DPDA (270 nN) was less than that on the glass (300 nN). Because the DPDA is less hydrophilic than glass, the glass surface will accumulate a larger water content. This water will, therefore, produce an increase in the net adhesive forces due to capillary force contributions. Experiments were also done in liquid,

demonstrating a reduction of adhesion due to the absence of a capillary contribution. In these liquid studies, van der Werf performed adhesion maps on gold films covered by a self-assembling monolayer. As the liquid medium was varied, the adhesion force was observed to change. These results were in agreement with observations found by Hoh *et al.* [24] who showed that adhesion forces should be diminished by adding ions to the solution. A similar approximation can also be seen in the work of Hans-Ulrich Krotil *et al.* [25].

The experiments described above can be categorized as "force-volume" and "pulsed-force microscopy" (as is defined by de Pablo *et al.* [26]). In force-volume mode (Koleske), the entire force curves are stored during imaging and the relevant parameters are determined during post-acquisition processing. In pulsed-force microscopy (Mizes, van der Werf) the physically-interesting data are extracted from the force curves during the imaging process. In the remainder of this paper, a new technique for performing quantitative, real-time force mapping is discussed in detail. This mode of adhesion mapping is called Jump Mode (JM) Scanning Force Microscopy [27].

IV. JUMP MODE SCANNING FORCE MICROSCOPY

IV.1. Jump Mode Description

Simultaneous, real-time images of the sample topography and the lift-off force are performed in Jump Mode as illustrated in Figure 4, where the motion of the tip as a function of time along (a) the x-axis and (b) the z-axis is plotted. In addition, (c) the cantilever deflection recorded as the tip is moved along the z-axis is also illustrated. In (d), a schematic of the resulting force curve is shown.

The AFM tip is first brought into contact with the sample during the coarse approach, under feedback control, until the setpoint cantilever displacement is achieved. The feedback is then disabled, and a ramp to the z-piezo for the sample is applied, withdrawing the sample by a prescribed amount. With the tip in this position, the topography and adhesion maps can be performed. At each point on the image, the control unit ramps the z-piezo voltage to move the sample through a given distance, δ, *toward* the tip. This brings the tip into contact with

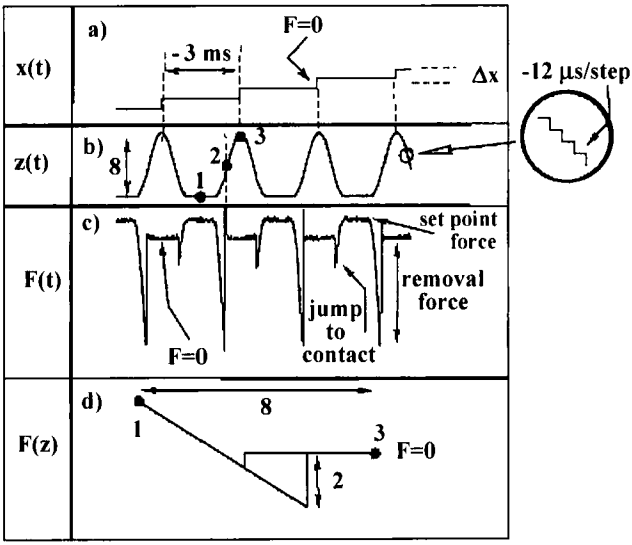

FIGURE 4 Oscilloscope traces showing (a) the position of the sample along the x-axis as a function of time, (b) the position of the sample along the z-axis as a function of time, (c) the normal force applied to the substrate by the tip as a function of time and (d) a schematic of the resulting force curve obtained during one cycle of the z-piezo.

the sample. The cantilever displacement is monitored during this process, providing the approach segment of the force curve. When the ramp is complete, the feedback is then enabled for a short time (typically 1 ms) and its output is stored as the topographic height. The feedback is then disabled, and an inverse ramp is applied to the z-piezo, withdrawing the tip from the sample. Again, the cantilever is monitored, providing the "withdrawal" portion of the force curve.

When the largest z value is reached (*i.e.*, the maximum tip – sample distance), a voltage step is applied to the x-piezo and the tip is quickly moved parallel to the surface. This allows motion without lateral force, and is similar to a "tapping-mode" scan. This process is repeated for all points in the image, providing topographic and force curve data at each point. The entire force curve at each point is, however, not stored in memory. Storing such data would significantly slow the scanning speed and require large amounts of memory. After each force curve has been completed, the relevant local parameters (such as lift-off force or elastic modulus) are extracted from the force

curve, and only these values are stored in memory. Following this approach, an entire adhesion map consisting of 256×256 data points takes about 10 minutes to complete.

In order to perform quantitative adhesion maps in real time, it is important to optimize the system's performance. Since the modulation of the z-position during force curves in Jump Mode is typically performed by ramping at a frequency of 1 kHz, resonant frequencies can easily be excited in the system. In order to prevent these excitations, a sine wave ramp is applied to the z-piezoelectric driver. The frequency of the sinusoidal ramp is chosen away from the resonance frequencies of the system.

IV.2. Comparison of Jump Mode with Other Adhesion Mapping Modes

Jump Mode combines the features of lift mode, of intermittent contact (tapping) mode scanning, of pulsed-force mode, as well as force-volume. As in the last three modes, in JM the lateral displacement of the tip and sample is done when they are not in contact, thus avoiding shear forces and the corresponding damage to tip and sample. As in force-volume mode, tip-sample interaction is measured at each point. However, in JM the interaction is evaluated and characterized usually by one parameter, which is displayed as an image in real time. The advantages of JM compared with force-volume are, on the one hand, a dramatic reduction of stored data and, on the other hand, its direct visualization without the need for post-acquisition processing. JM is similar to lift mode, since in both cases topography and tip-sample interaction are measured in different phases of an acquisition cycle. In JM, one cycle is performed at every image point, whereas, in lift mode, a whole scan line is acquired in a cycle. This implies that tip-sample distance is much better controlled in JM, since it is "refreshed" at every point after feedback is performed. In lift mode, this happens only after each scan line and, in fact, it has been observed that this distance varies along one scan line, presumably due to piezo creep, hysteresis, and/or cross talk between different piezotube axes. Finally, pulsed-force microscopy can be considered a special application of JM to measure adhesion, even though data processing is performed by analog electronics, as opposed to digital processing in the case of JM.

IV.3. Jump Mode Applications

Two different AFM heads were used to perform the following experiments presented here. The first AFM is a commercially-available instrument from Nano Tec^{TM} which features a modular design, easy adjustment of the optical system, top view of the AFM scanning region which makes it easy for optical microscope inspection, low thermal drift and a humidity-controlled system. The scanning range is up to $50\,\mu m \times 50\,\mu m$. The cantilever deflection was monitored by a laser beam deflection system. The system uses a large piezotube to minimize hysteresis effects. SiN_3 pyramidal cantilevers from Olympus ($k \sim 0.4$ N/m) were used in the system.

The second system has been described previously [28, 29] and is mounted in a small stainless steel vacuum chamber, allowing for control of environmental conditions. To avoid problems associated with absorbed water, the system was repeatedly pumped out to pressures of 20 mTorr, followed by a backfill with dry nitrogen gas. To study the effects of ambient conditions on adhesion, the system could be vented to the atmosphere. Si ultracantilevers from Park Scientific ($k \sim 2.0$ N/m) were used in the system.

Several procedures have been followed during these adhesion studies. Briefly, detection of the AFM cantilever displacement is performed using laser deflection techniques. Calibration of the cantilever's spring constant is performed by measuring the resonance frequency and using manufacturer-specified parameters such as length, width, elastic modulus, and density to calculate the spring constant [30]. In the second AFM system, a second laser deflection system is used to monitor the motion of the sample piezoelectric tube. This is critical for eliminating nonlinearities and creep when performing force measurements.

Both AFMs were controlled by a PC-based Nano Tec^{TM} control unit. This system of hardware and software controls all aspects of data acquisition, processing, and feedback, and is now a standard feature of the Nano Tec^{TN} software package. The core of the system is a Digital Signal Processor (DSP) with 4 simultaneous ADC/DAC channels, each with 16-bit accuracy. The DAC outputs drive a high-voltage amplifier unit which provides the scanning signals. Control and data signals are input through the ADC channels. Scanning and force

measurements are performed in real time under the execution of a C program which resides in the DSP memory.

V. RESULTS

Adhesion maps have been performed on a wide variety of different materials to explore fully the capabilities of this new technique. The following are a few selected examples.

V.1. Single-walled Carbon Nanotubes on SiO_2

As an example of adhesion mapping using Jump Mode, topographic and adhesion images were obtained on single-walled carbon nanotubes placed on a flat SiO_2 substrate. A sample of the results is shown in Figure 5. Simultaneous images of topography and adhesion are shown for a 250 nm × 250 nm area. The adhesion map shows three distinct regions with different adhesive characteristics. On the SiO_2 substrate, the adhesion is observed to be relatively constant, with slight changes in removal force appearing due to surface roughness. The removal force on the nanotubes is observed to be significantly less than that of the SiO_2 substrate (2 nN difference). A third region observed in the adhesion image is an area of high adhesion on either side of the carbon nanotubes. These results can be understood by applying the Derjaguin approximation [31, 32] which describes the interaction force $F(D)$ between two spherical bodies in close proximity (contact) as a function of separation distance, D.

$$F(D) = W\left(\frac{1}{C_t + C_s}\right) \tag{1}$$

Here, we see that the adhesion force will be a function of two factors: (a) the local geometry of the tip and surface (represented by the curvature of the tip, C_t, and the curvature of the sample, C_s), and (b) all other factors including chemical composition (represented in the form of W, the energy per unit area of two flat surfaces at separation D). From a purely geometric perspective, if the tip is located on a perfectly flat surface, $C_s = 0$. If the tip is located on top of a region

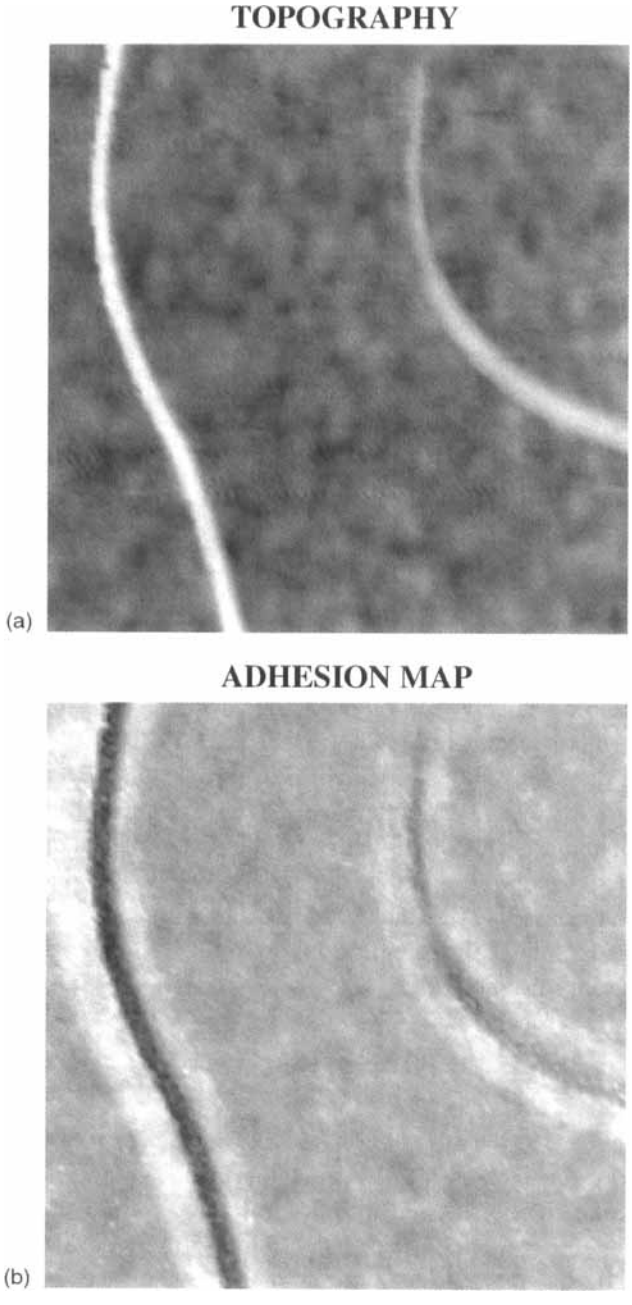

FIGURE 5 (a) Topography and (b) Adhesion map of single-walled carbon nanotubes on a silicon oxide substrate. (See Color Plate IV).

with positive surface curvature (such as on top of the nanotube), then Eq. (1) predicts that the adhesion force will be smaller than over the flat area. Conversely, if the curvature of the surface is negative (when the tip is on the side of the nanotube), the adhesion force will be greater. Therefore, the observations in the adhesion map can be qualitatively understood from these geometric considerations. Additionally, the chemical composition of the surfaces will also be a factor. The surface free energy for graphite is lower than that of silicon oxide, which, again, will act to produce a lower adhesion on the nanotube.

V.2. Au Bridge on Glass

In order to investigate further the effects of surface roughness and composition on adhesion maps, two thin gold electrodes were thermally evaporated onto a clean glass slide in such a way as to form two separate electrical contact pads, each 60 nm thick and separated by $\sim$10 μm. A nominal 30 nm thick Au film was then evaporated through a mask positioned at right angles to these electrodes to form a thin electrical connection (*i.e.*, a bridge) between the two contact pads.

Both topography and adhesion maps were obtained in the region of the Au bridge as shown in Figure 6. It is clear from a careful examination of the topographic images that the roughness of the Au film increases in proportion to the thickness. It is interesting to see how this surface roughness influences the adhesion. An analysis of the relevant adhesion maps permits this study to be performed. Adhesion maps show that the adhesion (*i.e.*, lift-off force) increases as the gold surface becomes rougher. In addition, clear evidence for a local decrease in adhesion due to particulate contamination of the glass substrate is also evident in Figure 6.

The variation in adhesion was quantitatively determined by calculating the RMS roughness and average adhesion force in the three relevant areas. These results are shown in Table I. As was observed qualitatively, a clear correlation is observed between the surface roughness and the adhesion force.

It is also instructive to examine the distribution of heights and adhesion forces over the entire images from Figure 6. The topography and adhesion histograms are shown in Figure 7. An examination of

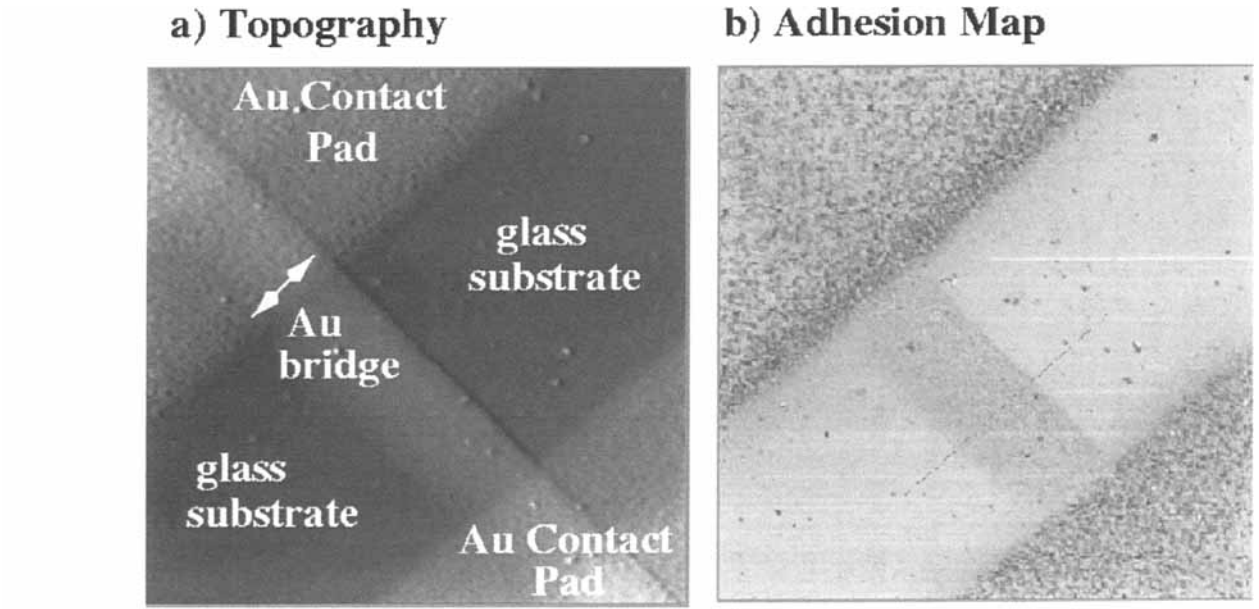

FIGURE 6 (a) A 10 μm × 10 μm AFM topographic scan (contact mode) of two Au contact pads spanned by a thin Au bridge supported on a glass substrate. In (b), an adhesion map of the same region. A mapping algorithm was used such that a lighter color (grey-scale in B & W) implies a larger adhesion force. (See Color Plate V).

TABLE I Quantitative comparison of topographic and adhesion force variations

RMS roughness	*Contact pad*	*Gold bridge*	*Glass substrate*
Topography (nm)	7.1	3.5	2.7
Adhesion force (a.u.)	619	278	202

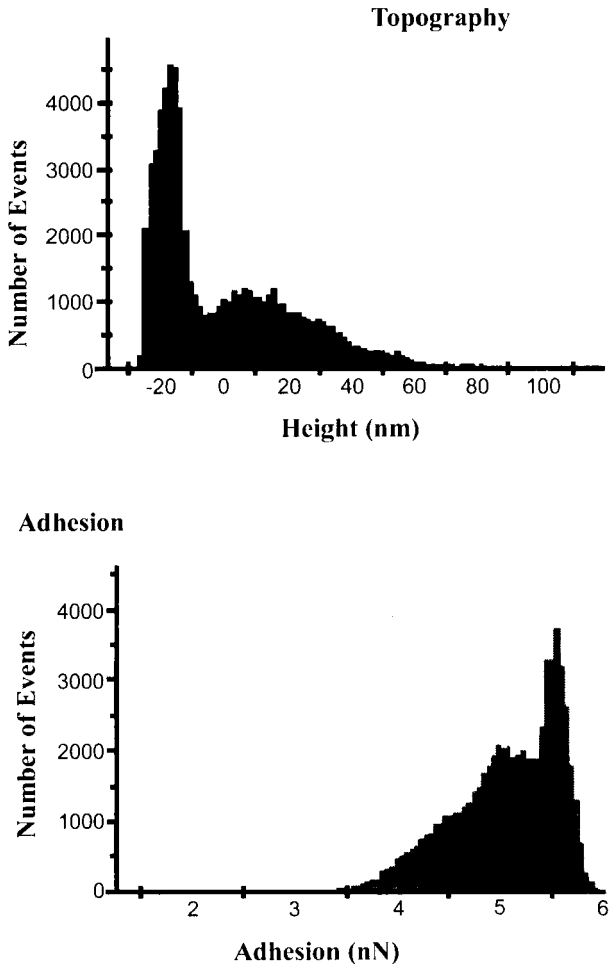

FIGURE 7 A histogram from the images shown in Figure 8 displaying the distribution of heights and lift-off forces.

the topographic histogram shows two features which represent (1) the glass surface (centered at -20 nm) and (2) the Au bridge plus the Au pads (centered around $\sim 30-40$ nm). The spread in height measured from the Au contact pad is evident and indicates a greater roughness characterizing this thicker Au film. By contrast, the glass substrate is smoother, as can be seen by the narrower peak in the topographic histogram.

The adhesion histogram also reveals two features that can be identified with the same topographic features. The adhesion between the glass substrate and AFM tip was found to require on average a 5.5 nN lift-off force. Because of the smoothness of the glass substrate, we believe the adhesion is dominated by the inter-molecular forces acting between the tip and glass. The region of the histogram with adhesion forces ranging from approximately 5 to 5.3 nN corresponds to forces found on the gold bridge. Forces below 5 nm correspond to the region of the gold contact pad. The variation in force over the contact pad region is due to the large variation in surface roughness. From Figure 7, the adhesion force from the Au bridge is found to be more uniform than from the Au contact pads. This correlated with the smoother topography associated with the Au bridge.

V.3. Adhesion from an Argon – Ion Sputtered HOPG Substrate

It is clear that both topography and chemistry play an important role in determining the shape of an adhesion map. For this reason, it is useful to investigate a surface that minimizes the chemical effects to adhesion. Highly-ordered pyrolytic graphite (HOPG) is ideal for this purpose because it is atomically flat over large regions. Furthermore, due to the bonding of the carbon atoms to form graphite sheets, the surface of flat HOPG is known to be unreactive. However, if HOPG is roughened, the adhesion properties should change.

A roughened sample of HOPG was prepared to study the alteration of adhesion due to surface roughness. An HOPG sample was masked in such a way so as to expose approximately one-half of the surface to an Argon – ion discharge for approximately 10 minutes at an Argon pressure of $\sim 10^{-3}$ Torr with the sample biased at a potential of 1000 V with respect to ground. The boundary region demarcating the

part of the surface exposed to the discharge and that covered by the mask was then investigated both in the topography and adhesion map modes. The results are shown in Figure 8 which shows three maps of both the topography and adhesion near the interface region. A histogram analysis allows the quantitative determination of the roughness by measuring the standard deviation in topography and the average lift-off force from the adhesion map. These values are listed under the three images. A clear correlation between increasing roughness and adhesion can be established in this way.

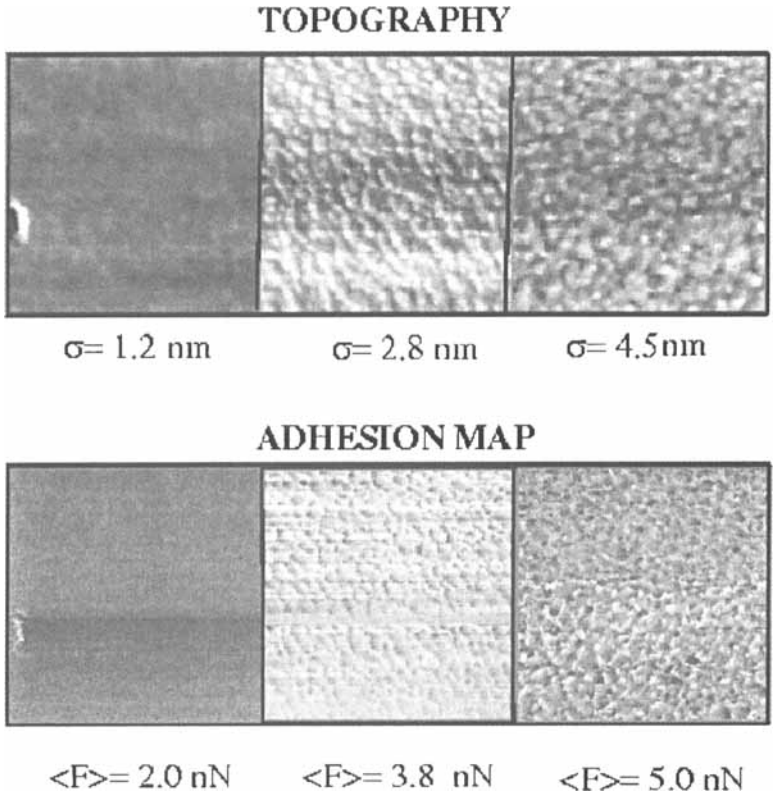

FIGURE 8 Three images, each spanning 1 μm × 1 μm, of an HOPG surface exposed to an Argon ion discharge for 10 minutes. Values for the roughness (calculated from the standard deviation of the topographic image (σ)) and the average lift-off force ($\langle F \rangle$) (acquired from the adhesion map) are listed. A quantitative correlation between substrate roughness and adhesion can be estimated in this way. (See Color Plate VI).

VI. CONCLUSION

The Atomic Force Microscope has developed into a quantitative tool for the measurement of adhesion forces between materials with nanometer-scale lateral resolution. Exploiting this ability, adhesion maps have been produced using a new technique called Jump Mode to study the adhesion force as a function of position on a material. This technique utilizes a DSP to acquire, process, and store topographical and adhesion data during AFM operation. Jump mode accommodates fast data acquisition rates, does not require large amounts of memory for data storage, and can be modified through software for other applications. This imaging method requires only the electronics required to perform contact-mode imaging. Additionally, lateral forces are virtually eliminated, so that mapping of delicate samples with high resolution in air and fluids is easily possible. Experiments were performed on a variety of materials to illustrate the effects of surface roughness and material composition on adhesion.

Acknowledgements

The authors would like to thank S. Howell and R. Reifenberger (Purdue University) and D. Rimai (Nexpress) for many helpful comments and suggestions. Additionally, the authors would like to thank P. J. de Pablo, J. Colchero, and A. M. Baro for their contributions toward this work. The work in Madrid was supported by project CICYT PB95-0169. The work at Purdue was partially funded by the Office of Imaging Division of Eastman Kodak.

References

[1] Binnig, G., Quate, C. F. and Gerber, Ch., *Phys. Rev. Lett.* **56**, 930 (1986).
[2] Hao, H. W., Baro, A. M. and Saenz, J. J., *J. Vac. Sci. Technol.* **B9**(2), 1323 (1991).
[3] Abraham, D. W., Williams, C. C. and Wickramasinghe, H. K., *Microscopy* **152**, 863 (1988).
[4] Ducker, W. A., Senden, T. J. and Pashley, R. M., *Nature* (London) **353**, 239 (1991).
[5] Gady, B., Schleef, D., Reifenberger, R., DeMejo, L. P. and Rimai, D. S., *Phys. Rev. B* **53**, 8065 (1996).
[6] Meyer, E., Overney, R., Howard, L., Brodbeck, D., Luthi, R. and Guntherodt, H. J., In: *Fundamentals of Friction: Macroscopic and Microscopic Processes*, Singer, I. L. and Pollock, H. M. (Eds.) (Kluwer Academic Publishers, Netherlands, 1992), pp. 427–436.

[7] Schaefer, D. M., Carpenter, M., Reifenberger, R., DeMejo, L. P. and Rimai, D. S., *J. Adhesion Sci. Technol.* **8**, 197 (1994).
[8] Mizes, H. A., *J. Adhes. Sci. Technol.* **8**, 937 (1994).
[9] Rugar, D. and Hansma, P., *Physics Today*, p. 23 Oct. (1990).
[10] Koshiba, K., Tanaka, I., Nakamura, Y., Nobe, H. and Sakaki, H., *Appl. Phys. Lett.* **70**, 883 (1997).
[11] Binnig, G. K., *Physica Scripta* **T19**, 53 (1987).
[12] Drake, B., Prater, C. B., Weisenhorn, A. L., Gould, S. A., Albrecht, T. R., Quate, C. F., Cannell, D. S., Hansma, H. G. and Hansma, P. K., *Science* **243**, 1586 (1989).
[13] Schaefer, D. M., Carpenter, M., Reifenberger, R., DeMejo, L. P. and Rimai, D. S., *J. Adhesion Sci. Technol.* **8**, 197 (1994).
[14] Schaefer, D. M., Carpenter, M., Gady, B., Reifenberger, R., DeMejo, L. P. and Rimai, D. S., *J. Adhesion Sci. Technol.* (1995).
[15] Lee, G. U., Kidwell, D. A. and Colton, R. J., *Langmuir* **10**(2), 354 (1994).
[16] Schaefer, D. M., Carpenter, M., Gady, B., Reifenberger, R., DeMejo, L. P. and Rimai, D. S., *J. Adhesion Sci. Technol.* **9**, 1049 (1995).
[17] Johnson, K. L., Kendall, K. and Roberts, A. D., *Proc. R. Soc. London* **A324**, 301 (1971).
[18] Mizes, H. A., Loh, K. G. R., Miller, J. D., Ahuja, S. K. and Grabowski, E. F., *Appl. Phys. Lett.* **59**, 22, 2901 (1991).
[19] Gady, B., Reifenberger, R., Rimai, D. S. and DeMejo, L. P., *Langmuir* **13**, 2533 (1997).
[20] Gady, B., Reifenberger, R. and Rimai, D. S., *J. Appl. Phys.* **84**, 319 (1998).
[21] Schaefer, D. M., Unpublished.
[22] Koleske, D. D., Lee, G. U., Gans, B. I., Lee, K. P., Dilella, D. P., Wahl, K. J., Barger, W. R., Withman, L. J. and Colton, R. J., *Rev. Sci. Instrum.* **66**, 9, 4566 (1995).
[23] van der Werf, K. O., Putman, C. A., de Grooth, B. G. and Greve, J., *Appl. Phys. Lett.* **65**, 9, 1194 (1994).
[24] Hoh, J. H., Cleveland, J. P., Prater, C. B., Revel, J. P. and Hansma, P. K., *J. Amer. Chem. Soc.* **114**, 4917 (1992).
[25] Hans-Ulrich Krotil, J., Stifer, T., Waschipky, H., Weishaupt, K., Hild, S. and Marti, O., *Surf. Interface Anal.* **27**, 336–340 (1999).
[26] de Pablo, P. J., Colchero, J., Gomez-Herrero, J. and Baro, A. M., *Appl. Phys. Lett.* **73**, 22, 3300 (1998).
[27] de Pablo, P. J., Colchero, J., Gomez, J., Baro, A. M., Schaefer, D. M., Howell, S., Walsh, B. and Reifenberger, R., *J. Adhesion* to be published.
[28] Mahoney, W., Schaefer, D. M., Patil, A., Andres, R. P. and Reifenberger, R., *Surf. Sci.* **316**, 383 (1994).
[29] Schaefer, D. M., Andres, R. P. and Reifenberger, R., *Phys. Rev. B* **51**, 5322 (1995).
[30] Sarid, D., *Scanning Force Microscopy* (Oxford University press) (1991).
[31] Mizes, H. A., *J. Adhesion* **51**, 155 (1995).
[32] Israelachvili, J. N., *Intermolecular and Surface Forces* (Academic Press, London, 1985), pp. 130–133.